

# Moderately Supervised Learning: Definition, Framework and Generality

Yongquan Yang (remy\_yang@foxmail.com)

## Abstract

Supervised learning (SL) has achieved remarkable success in numerous artificial intelligence (AI) applications. In the current literature, by referring to the properties of the ground-truth labels prepared for the training data set, SL is roughly categorized as fully supervised learning (FSL) and weakly supervised learning (WSL). FSL concerns the situation where the training data set is assigned with ideal ground-truth labels, while WSL concerns the situation where the training data set is assigned with non-ideal ground-truth labels. However, solutions for various FSL tasks have shown that the given ground-truth labels are not always learnable, and the target transformation from the given ground-truth labels to learnable targets can significantly affect the performance of the final FSL solutions. Without considering the properties of the target transformation from the given ground-truth labels to learnable targets, the roughness of the FSL category conceals some details that are critical to building the appropriate solutions for some specific FSL tasks. Thus, for engineers in the AI application field of FSL, it is desirable to reveal these details. This article attempts to achieve this goal by expanding the categorization of FSL and investigating the sub-type that plays the central role in FSL. More specifically, taking into consideration the properties of the target transformation from the given ground-truth labels to learnable targets, we firstly categorize FSL into three narrower sub-types and then focus on the sub-type moderately supervised learning (MSL) that concerns the situation where the given ground-truth labels are ideal, but due to the simplicity in annotation of the given ground-truth labels, careful designs are required to transform the given ground-truth labels into learnable targets. From the perspectives of the definition, framework and generality, we comprehensively illustrate MSL to reveal what details are concealed by the roughness of the FSL category. At the meantime, via presenting the definition, framework and generality of MSL, this paper as well establishes a tutorial for AI application engineers to refer to viewing a problem to be solved from the mathematician's vision.

## 1. Introduction

With the development of fundamental machine learning techniques, especially deep learning [1], supervised learning (SL) has achieved great success in various classification and regression tasks for artificial intelligence (AI) applications. Typically, a predictive machine learning model is learned from a training data set that contains a number of training examples. For SL, a training example usually consists of an event/entity and its correspondingly given ground-truth label. In classification, the ground-truth label indicates the class to which its associated event/entity belongs; in regression, the ground-truth label is a real-value response corresponding to the event/entity. There are two main streams in the current SL literature: fully supervised learning (FSL) and weakly supervised learning (WSL) [2]. FSL focuses on the situation where the training data set is assigned with ideal (complete, exact and accurate) ground-truth labels. In contrast, WSL focuses on situations where the training dataset is assigned with non-ideal (incomplete, inexact or inaccurate) ground-truth labels. The clear boundary between FSL and WSL is the properties (completeness, exactness and accuracy) of the ground-truth labels prepared for the training examples.

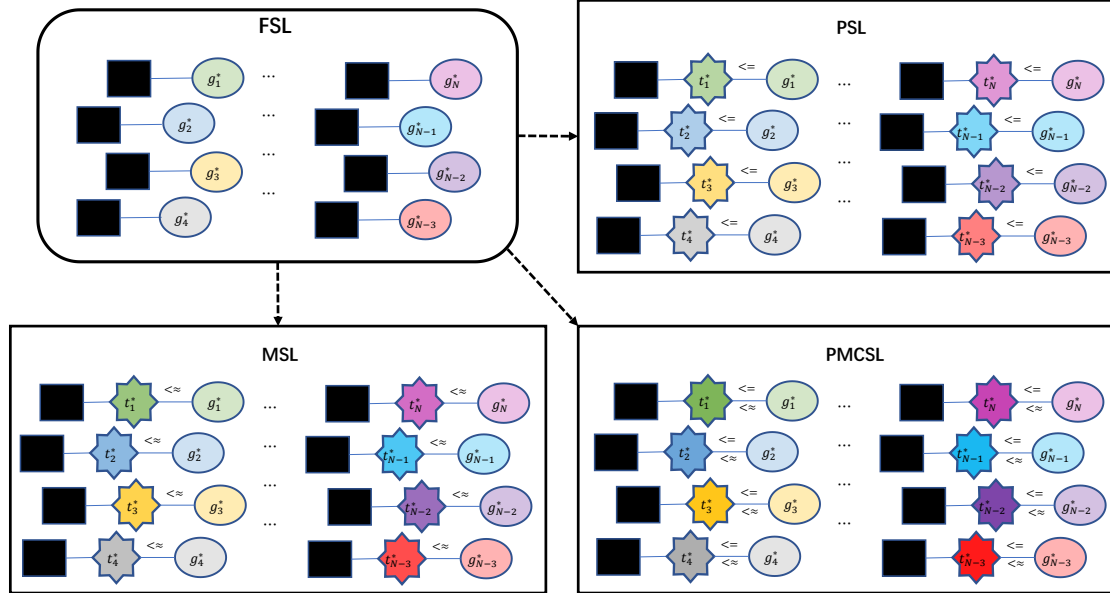


Fig. 1. Narrower categorization for fully supervised learning (FSL). The three sub-types of FSL include precisely supervised learning (PSL), moderately supervised learning (MSL), and precisely and moderately combined supervised learning (PMCSL). Black rectangles denote events/entities in the training data set; coloured ellipses indicate the ground-truth labels assigned to corresponding events/entities; coloured polygons signify learnable targets transformed from corresponding ground-truth labels.  $\leq$ / $\approx$  denote 'carelessly designed' or 'carefully designed' target transformation.

However, in many real-world practice FSL tasks, we cannot directly learn a predictive model that can map from events/entities in the training examples to their correspondingly given ground-truth labels. The main reason for this situation lies in the fact that the given ground-truth labels are not always learnable though ideal are they. We must first construct a target transformation from the given ground-truth labels into structured learnable targets, and then learn a predictive model that maps the events/entities in the training examples to their corresponding learnable

targets. Existing solutions for various FSL tasks have shown that the target transformation from the given ground-truth labels to the learnable targets can significantly affect the performance of the final FSL solution [3–7]. By simply referring to the properties of the ground-truth labels prepared for the training examples without considering the properties of the target transformation, the roughness of the FSL category conceals some details that can be critical to building the appropriate solutions for some specific FSL tasks. Thus, for practitioners in the application field of FSL, it is desirable to reveal these details. This article attempts to achieve this goal by expanding the categorization of FSL and investigating the central sub-type of FSL.

Defining the properties of the target transformation for an FSL task as ‘carelessly designed’ and ‘carefully designed’ two types, we further categorize FSL into three narrower sub-types. The three sub-types include precisely supervised learning (PSL), moderately supervised learning (MSL), and precisely and moderately combined supervised learning (PMCSL). A short illustration for this narrower categorization is presented in Fig. 1. PSL concerns the situation where the given ground-truth labels are precisely fine. In this situation, we can carelessly design a target transformation to obtain the learnable targets from the given ground-truth labels. In other words, to some extent, the given ground-truth labels can be directly viewed as learnable targets. PSL is the most classic sub-type of FSL, and typical tasks include simple task like image classification [8] and complicated task like image semantic segmentation [9]. MSL concerns the situation where the given ground-truth labels are ideal, but due to the simplicity in annotation of the given ground-truth labels, careful designs are required to transform the given ground-truth labels into learnable targets for the learning task. This situation is different from the classic PSL since the given ground-truth labels must be carefully transformed into learnable targets for the learning task, which would otherwise lead to poor performance. This situation is also different from WSL since the given ground-truth labels are not incomplete, inexact or inaccurate but ideal. We refer to this situation as an issue of moderately supervised learning (MSL), since the given ground-truth labels for the learning task are not as strong as for PSL or as weak as for WSL. Typical MSL tasks include cell detection (CD) [3] and line segment detection (LSD) [4]. PMCSL concerns the situation where the given ground-truth labels contain both precise and moderate annotations. Usually, PMCSL consists of a few PSL and MSL sub-tasks, thus the target transformation for this situation requires both careless designs and careful designs. Typical PMCSL tasks include visual object detection [10], facial expression recognition [11] and human pose identification [12].

In the three narrower sub-types, PSL only counts for a small proportion of FSL, for simple tasks (such as image classification) of PSL are very few in FSL and complicated tasks (such as image semantic segmentation) of PSL usually requires precisely fine ground-truth labels which are labour extensive. However, MSL counts for the majority of FSL, due to the fact that the ground truth labels required by MSL are simple in annotation and MSL is an essential part of PMCSL which account for the majority of FSL. As a result, MSL plays the central role in the field of FSL. Although solutions have been intermittently proposed for different MSL tasks, currently, insufficient researches have been devoted to clearly defining and systematically analysing MSL, so as to reveal the details concealed by the roughness of the FSL category. To fill in this gap, we present comprehensive elaborations for MSL from the perspectives of definition, framework and generality. In this paper, we formulate MSL to clearly define it and present a generalized framework to systematically analyse MSL. In addition, we also show the generality exist among different MSL solutions; that is, solutions for a wide variety of MSL tasks can be abstractly unified into the presented MSL

framework. Eventually, based on the definition, framework and generality presented for MSL, we discuss the key points of constructing fundamental MSL solutions and the key problems of developing better MSL solutions, to reveal some details that are critical to building the appropriate solutions but concealed by the roughness of the FSL category.

As an application engineer who uses deep learning technology to promote the development of AI applications, in addition to chasing the state-of-the-art result for a problem to be solved, viewing the problem from the mathematician's vision is as well critical to discover, evaluate and select appropriate solutions for the problem, especially when deep learning has been becoming increasingly standardized and reaching its limits in many AI applications. However, currently, most AI application engineers primarily focus on chasing the state-of-the-art results for a problem to be solved, and few of them pay attention to viewing the problem from the mathematicians' vision. So, the question is how is the mathematicians' vision? There is a generalized answer to this question, which has been presented by the Chinese mathematician Jingzhong Zhang [13]: "Mathematicians' vision is abstract. Those we think are different, they seem to be the same. Mathematicians' vision is precise. Those we think are the same, they seem to be very different. Mathematicians' vision is clear and sharp. They continue pursuing mathematical conclusions that we feel very satisfied with. Mathematicians' vision is dialectical. We think one is one and two is two, but they often focus on what is unchanging in the changing and what is changing in the unchanging." Via presenting the definition, framework and generality of MSL, this paper as well establishes a specific example for understanding of this generalized answer, which can be a tutorial for AI application engineers to refer to viewing a problem to be solved from the mathematician's vision.

## 2. Preliminary

Formally, a supervised learning (SL) task is to learn a function  $f: d \mapsto g^*$  from a training data set  $\mathcal{T}$ . Usually,  $d$  denotes a set of events/entities,  $g^*$  represents the given ground-truth labels corresponding to  $d$ , and the training dataset  $\mathcal{T}$  consists of the events/entities  $d$  with their ground-truth labels  $g^*$ . In the current literature, there are two main types of SL: FSL and WSL. Usually, these two types are distinguished according to the completeness, exactness and accuracy of the ground-truth labels prepared for the training data set  $\mathcal{T}$ . Some basic notations that appear in this paper are summarized in Table 1.

### 2.1 Fully supervised learning

FSL learns predictive models with complete, exact and accurate ground-truth labels. Specifically, the training data set  $\mathcal{T} = \{(d_1, g_1^*), \dots, (d_N, g_N^*)\}$ , where  $N$  is the number of events/entities and each  $d_n$  has a label  $g_n^*$  that can ideally describe its ground-truth. Based on such prepared training data sets, FSL has been widely adopted to solve many fundamental SL tasks such as image classification, visual object tracking, visual object detection, and image semantic segmentation in the field of computer vision [14–17].

### 2.2 Weakly supervised learning

WSL attempts to learn predictive models with incomplete, inexact or inaccurate ground-truth labels [18]. Learning with incomplete ground-truth labels focuses on the situation where only a small amount of ideally labelled data is given to train a predictive model, while abundant unlabelled data are available. In this situation, the ideally labelled data are insufficient to learn a good model. Active learning [19] and semi-supervised learning [20] are two typical techniques for

this situation. Specifically, the training data set  $\mathcal{T} = \{(d_1, g_1^*), \dots, (d_J, g_J^*), d_{J+1}, \dots, d_N\}$ , where only a small portion  $\{d_j | j \in \{1, \dots, J\}\}$  of  $d$  has ground-truth labels. Learning with inexact ground-truth labels concerns using only coarsely labelled data that is not as exact as the ideally labelled data to learn a predictor. The typical technique for this situation is multi-instance learning [21]. Specifically, the training data set  $\mathcal{T} = \{(d_1, g_1^*), \dots, (d_N, g_N^*)\}$ , where  $d_n = \{d_{n,1}, \dots, d_{n,M_n}\} \subseteq d$  is called a bag,  $d_{n,m} \in d$  ( $m \in \{1, \dots, M_n\}$ ) is an instance, and  $M_n$  is the number of instances in  $d_n$ . For a two-class classification multi-instance learning task where  $t^* = \{y, n\}$ ,  $d_n$  is a positive bag, i.e.,  $t_n^* = y$ , if there exists  $d_{n,p}$  that is positive, while what is known is only  $p \in \{1, \dots, M_n\}$ . The goal is to predict labels for unseen bags. Learning with inaccurate ground-truth labels focuses on using data the labels of which compared with the ideal ground-truth labels may contain errors to train a reasonable predictive model. A typical technique for this situation is learning with noisy labels [22]. Specifically, the training data set  $\mathcal{T} = \{(d_1, (g_1^* + \Delta_1)), \dots, (d_N, (g_N^* + \Delta_N))\}$ , where  $(g_n^* + \Delta_n)$  is the given ground-truth label, which consists of an accurate label  $g_n^*$  and a label error  $\Delta_n$ . With the efficiency and lower cost of the data labelling process, WSL has become popular for addressing many complicated SL tasks that requires labour extensive annotations.

Table 1. Summary of basic notations used in this paper.

Notation	Meaning
$f$	a function that maps from $a$ to $b$
$\mathcal{T}$	a training data set that consists of events/entities with ground-truth labels
$d$	a set of events/entities
$g^*$	Ground-truth labels corresponding to events/entities
$N$	number of events/entities in the training data set $\mathcal{T}$
$t^*$	learnable targets, a transformation of $g^*$
$\leq / \approx$	non-parameterized/parameterized transformation
$\wedge / \vee$	and/or
$t$	predicted targets of events/entities
$g$	final predicted labels, a re-transformation of $t$
$I$	space of learnable targets $t^*$
$J$	space of predicted targets $t$
$H$	space of final predicted labels $g$
$\omega^d / \omega^i / \omega^e$	parameters for Decoder/Inferencer/Encoder
$M^d / M^i / M^e$	space of parameters for Decoder/Inferencer/Encoder
$\mathcal{F}$	a 2D image lattice
$p$	a 2D point in image lattice $\mathcal{F}$
$P$	a set of cell centres labelled in $\mathcal{F}$
$L$	a set of line segments labelled in $\mathcal{F}$
$D$	an input image lattice

### 3. Narrower Sub-types of Fully Supervised Learning

The categorization in the preliminary section simply takes into consideration the properties (completeness, exactness and accuracy) of the ground-truth labels prepared for the training data

set. However, in practice, we usually cannot directly learn a function  $f: d \mapsto g^*$  for an FSL task. We must build a target transformation from given ground-truth labels  $g^*$  to learnable targets  $t^*$ , and learn a function  $f: d \mapsto t^*$ . In this section, by taking the properties of the target transformation from  $g^*$  to  $t^*$  into consideration, we expand the categorization for FSL. Usually, a target transformation for an FSL task is coupled with a label re-transformation from the predicted targets of the learnt function  $f$  to the final predicted labels. Since a label re-transformation commonly consists of the reverse operations corresponding to its coupled target transformation, in this section, we assume that the properties of the label re-transformation remain the same as the properties of its coupled target transformer and give no additional discussions.

### 3.1 Properties of target transformation

We classify the target transformations of solutions for FSL tasks into ‘carelessly designed’ and ‘carefully designed’ two types. Intrinsically, we define that a target transformation is the ‘carelessly designed’ type if it is non-parameterized while a target transformation is ‘carefully designed’ type if it is parameterized, due to the fact that a non-parameterized target transformation simply requires careless designs while a parameterized transformer must require careful designs. That a non-parameterized target transformation simply requires careless designs is because it can generate a type of the learnable targets that can be considered to be optimal. However, that a parameterized target transformation must require careful designs is because adjusting its parameters can generate various types of learnable targets from which the optimal type of learnable targets need to be found. To formally summarize the properties of a target transformation, we present Definition 1 as follow.

**Definition 1.** *For the given ground-truth labels  $g^*$ , the learnable targets generated by a ‘carelessly designed’ transformation are*

$$t^* = \{t_n^* | t_n^* \leq g_n^*, n \in \{1, \dots, N\}\},$$

*where  $\leq$  signifies the non-parameterized transformation of  $t_n^*$  from  $g_n^*$  and the type of targets  $t^*$  can be considered as optimal; and the learnable targets generated by a ‘carefully designed’ transformation are*

$$t^* = \{t_n^* | t_n^* \lesssim g_n^*, n \in \{1, \dots, N\}\},$$

*where  $\lesssim$  signifies the parameterized transformation of  $t_n^*$  from  $g_n^*$  and the optimal type of targets  $t^*$  need to be found by adjusting the parameters.*

### 3.2 Sub-types of FSL

Taking into consideration the two properties of a target transformation presented in Definition 1, we further classify FSL into three narrower sub-types: precisely supervised learning (PSL), moderately supervised learning (MSL), and precisely and moderately combined supervised learning (PMCSL).

#### 3.2.1 Precisely supervised learning

PSL concerns the situation where the given labels  $g^*$  in the training data set have precisely fine ground-truth labels. In this situation, we can simply construct a non-parameterized target transformation with careless designs to obtain the learnable targets  $t^*$  from  $g^*$ . Image classification [8] and image semantic segmentation [9] are two typical PSL problems.

In a  $C$ -class image classification task, the given ground-truth label for the class of an image can usually be transformed into a learnable target using a  $C$ -bit vector. In this vector, the bit

corresponding to the given ground-truth label is set to 1, and the remaining bits are set to 0. Similarly, for a  $C$ -class image semantic segmentation task, each pixel point in the given ground-truth label for the semantic objects in an image can be transformed into a value at the same pixel point in the learnable target. The transformed value can be a one-hot vector in classification or real-value response in regression, corresponding to its predefined class in the given ground-truth label. We can note that the target transformations for these two PSL tasks are non-parameterized and can be simply built with careless designs. In other words, to some extent, the given ground-truth labels  $g^*$  can be viewed as learnable targets due to their precise fineness.

### 3.2.2 Moderately supervised learning

MSL focuses on the situation where the given ground-truth labels  $g^*$  in the training dataset are ideal while possessing to some extent extreme simplicity. This situation is different from PSL since the simplicity of  $g^*$  makes directly learning from the learnable targets of its carelessly designed transformation probably impossible or leads to very poor performance. MSL is also different from WSL, as the given ground-truth labels are not incomplete, inexact or inaccurate but ideal. Since the given ground-truth labels are not strong enough for PSL but also not weak enough for WSL, we refer to this situation as MSL. Due to the simplicity of  $g^*$ , in this situation, the target transformation from  $g^*$  to learnable targets  $t^*$  usually is parameterized and must require careful designs. Cell detection (CD) [3] and line segment detection (LSD) [4] with point labels are two typical MSL tasks.

In the CD task, the given ground-truth labels for cells in an image lattice are simply a set of 2D points indicating the cell centres. In the LSD task, the given ground-truth labels for line segments in an image lattice are simply a set of tuples, each of which contains two 2D points. The connection between the two 2D points of a tuple indicates a line segment in an image lattice. As the given ground-truth labels for these two tasks are extremely simple, directly transforming them into learnable targets, in which pixel points corresponding to  $g^*$  are set as foreground objects and the rest are set as background objects, will make the learning task impossible or lead to very poor performance. A more appropriate target transformation which are restricted by a number of parameters (a parameterized target transformation) can be used to alleviate this situation. However, adjusting the parameters of this parameterized target transformation can result in various learnable targets that can significantly affect the performance of the final solution for an MSL task. As a result, it is usually difficult to find the optimal learnable targets from the parameterized target transformation for an MSL task. Thus, an appropriately parameterized target transformation for an MSL task must require careful designs to be constructed.

### 3.2.3 Precisely and moderately combined supervised learning

PMCSL concerns the situation where the given ground-truth labels  $g^*$  contain both precise and moderate annotations. In this situation, the target transformation is usually built to have a mixture of properties of both the target transformations designed for PSL and MSL tasks. Typical PMCSL tasks include visual object detection [10], facial expression recognition [11] and human pose identification [12]. Each of these tasks usually consists of a few PSL and MSL problems.

In the visual object detection task, the given ground-truth labels for the objects in an image lattice are usually a set of tuples, each containing a class name and a bounding box to indicate the category of an object and its position. Currently, deep convolutional neural network-based [8, 23–27] one-stage approaches (YOLO [28–31], SSD [32] and RetinaNet [6]) and two-stage approaches (RCNN [33], SPPNet [34], Fast RCNN [35], Faster RCNN [36] and FPN [5]) are the state-of-the art

solutions for this task. The target transformations of these solutions usually have a parameterized sub-transformation and a non-parameterized sub-transformation. The parameterized sub-transformation is responsible for pre-defining a set of reference boxes (a.k.a. anchor boxes) with different sizes and aspect ratios at different locations of an image lattice. The sizes and aspect ratios can be adjusted to generate various reference boxes. These reference boxes are used to indicate the probabilities of corresponding areas as objects in an image lattice. The non-parameterized sub-transformation is responsible for transforming the reference boxes obtained from the parameterized sub-transformation into their categories and locations according to the ground-truth class names and ground-truth bounding boxes labelled in an image lattice. In facial expression recognition [11] and human pose identification [12] tasks, the detection of landmarks of a face or a human is the primary problem. The given ground-truth labels for the landmarks of a face or a human in an image are usually a set of tuples, each of which contains a 2D vector and a number to indicate the position and category of the landmark. The target transformation of possible solution for the detection of landmarks also has a parameterized sub-transformation and a non-parameterized sub-transformation. Basically, the detection of landmarks consists of two sub-problems: locating the landmarks and classifying the located landmarks. The parameterized sub-transformation, which is similar to the target transformers of solutions for pure MSL problems, aims to generate targets for locating landmarks, and the non-parameterized sub-transformation is responsible for producing targets for classifying the located landmarks. These typical problems show that the target transformation for PMCSL enjoys a mixture of properties of the target transformations for pure PSL and pure MSL.

### 3.3 Analysis

In fact, the three sub-types (PSL, MSL and PMCSL) of FSL can be converted between each other by changing the modeling methods of the target transformations for their solutions. However, once the target transformation for a possible solution has been constructed, the sub-type of the corresponding FSL task is clearly clarified. In other words, the constructed target transformation of a possible solution for an FSL task fundamentally determines the sub-type of this FSL task, which is crucial to building the appropriate solution for the task.

Training Data Set		Target Transformer	
FSL	$\mathcal{T} = \{(d_1, g_1^*), \dots, (d_N, g_N^*)\}$	$t^* = \{t_n^*   t_n^* \leq g_n^*, n \in \{1, \dots, N\}\}$	PSL
		$t^* = \{t_n^*   t_n^* \leq \approx g_n^*, n \in \{1, \dots, N\}\}$	MSL
		$t^* = \{t_n^*   t_n^* \leq \wedge \leq \approx g_n^*, n \in \{1, \dots, N\}\}$	PMCSL
Incomplete	$\mathcal{T} = \{(d_1, g_1^*), \dots, (d_j, g_j^*), d_{j+1}, \dots, d_N\}$	$t^* = \{t_n^*   t_n^* \leq \vee \leq \approx g_n^*, n \in \{1, \dots, N\}\}$	WSL
Inexact	$\mathcal{T} = \{(d_1, g_1^*), \dots, (d_N, g_N^*)\},$ $d_n = \{d_{n,1}, \dots, d_{n,M_n}\} \subseteq d,$ $d_{n,m} \in d (m \in \{1, \dots, M_n\})$		
Inaccurate	$\mathcal{T} = \{(d_1, (g_1^* + \Delta_1)), \dots, (d_N, (g_N^* + \Delta_N))\}$		

Fig. 2. Deeper categorization for SL.  $\leq / \leq \approx$  denote non-parameterized ('carelessly designed') / parameterized



('carefully designed') target transformation.  $\wedge/V$  denote and/or.

Additionally, taking Definition 1 into consideration, WSL can also be classified into narrower sub-types. However, here we only focus more on the sub-types of FSL, since FSL is more fundamental than WSL in the field of SL and the sub-types of FSL can naturally adjust to WSL. As a result, a deeper categorization for SL is presented as Fig. 2.

## 4. Moderately Supervised Learning

In the three narrower sub-types, PSL only counts for a small proportion of FSL, for simple tasks (such as image classification) of PSL are very few in FSL and complicated tasks (such as image semantic segmentation) of PSL usually requires precisely fine ground-truth labels which are labour extensive. However, MSL counts for the majority of FSL, due to the fact that the ground truth labels required by MSL are simple in annotation and MSL is also an essential part of PMCSL which is widely existing in FSL. As a result, MSL plays the central role in the field of FSL. Currently, insufficient research has been devoted to comprehensively illustrate MSL, although solutions have been intermittently proposed for different MSL tasks. In this section, we comprehensively illustrate MSL from the perspectives of the definition, framework and generality, aiming to reveal the details that are critical to building the appropriate solutions but concealed by the roughness of the FSL category.

### 4.1 Definition

#### 4.1.1 Definition for FSL

Let us consider the situation where the given ground-truth labels of an amount of data are the ideal labels but possess simplicity. Specifically, with the given simple ground-truth labels  $g^*$ , the ultimate goal of the learning task here is to find the final predicted labels  $g$  that minimize the error against  $g^*$ . Regarding this situation as a classic FSL problem, we can define the objective function as

$$\min_g \ell(g, g^*), \quad (0-1)$$

where  $\ell(\cdot, \cdot)$  refers to a loss function that estimates the error between two given elements. The smaller the value of this function is, the better the found  $g$  is.

#### 4.1.2 Definition for MSL

Due to the simplicity of  $g^*$ , we must carefully build a target transformation that transforms  $g^*$  into learnable targets  $t^*$ . On the basis of the transformed learnable targets  $t^*$ , we build a learning function that maps events/entities  $t^*$  to the predicted targets and find those predicted targets  $t$  that minimize the error against  $t^*$ . Based on the found predicted targets  $t$ , we then carefully build a label re-transformation that re-transforms  $t$  into the final predicted labels and find those predicted labels  $g$  that can minimize the error against the ground-truth labels  $g^*$ . We assume  $t^*$  can be constructed by 'decoding'  $g^*$  as the learnable targets  $t^*$  are more informative than the ground-truth labels  $g^*$ , the predicted targets  $t$  can be obtained by 'inferring'  $d$ , and  $g$  can be constructed by 'encoding'  $t$  as the final predicted labels  $g$  are less informative than the predicted targets  $t$ . Formally, we specify the following definition for MSL:

$$\begin{aligned} t^* &= \text{decoder}(g^*) \quad t^* \in I, \\ t &= \text{inferrer}(d) \quad t \in J, \quad \min_{t \in J} \ell^i(t, t^*), \\ g &= \text{encoder}(t) \quad g \in H, \quad \min_{g \in H} \ell^e(g, g^*), \end{aligned} \quad (0-2)$$

where *decoder* denotes the target transformation, *inferred* denotes the learning function  $f$ , *encoder* denotes the label re-transformation, and  $I$ ,  $J$  and  $H$  denote the spaces of learnable targets  $t^*$ , predicted targets  $t$  and final predicted targets  $g$ .

#### 4.1.3 Analysis

Comparing Eq. (0-2) with Eq. (0-1), we can note that, by taking into consideration the properties of the target transformation from the given ground-truth labels to learnable targets, the definition specified for MSL proves that some details are indeed concealed by the rough definition for FSL.

## 4.2 Framework

On the basis of the specified definitions for MSL, in this section, we present a generalized MSL framework. The outline of the presented MSL framework is shown as Fig. 3, in which basic components for constructing a fundamental MSL solution and basic procedures of mutual collaborations among the basic components are depicted.

### 4.2.1 Basic component

**The decoder** transforms the given simple ground-truth labels  $g^*$  into learnable targets  $t^*$ . Commonly, the decoder is built on the basis of prior knowledge which is parameterized by  $\omega^d$ . Abstractly, we obtain the learnable targets  $t^*$  by

$$t^* = \text{decoder}(g^*; \omega^d). \quad (1)$$

**The inferrer** models the map between the events/entities  $d$  and corresponding learnable targets  $t^*$ . Usually, the inferrer is built on the basis of machine learning techniques and is parameterized by  $\omega^i$ . Abstractly, we obtain the predicted targets  $t$  by

$$t = \text{inferred}(d; \omega^i). \quad (2)$$

**The encoder** re-transforms the predicted targets  $t$  of the inferrer into the final predicted labels  $g$ . Coupled with the decoder, the encoder is built on the basis of the decoder's output  $t^*$  which is parameterized by  $\omega^e$ . Abstractly, we obtain the final predicted labels  $g$  by

$$g = \text{encoder}(t; \omega^e). \quad (3)$$

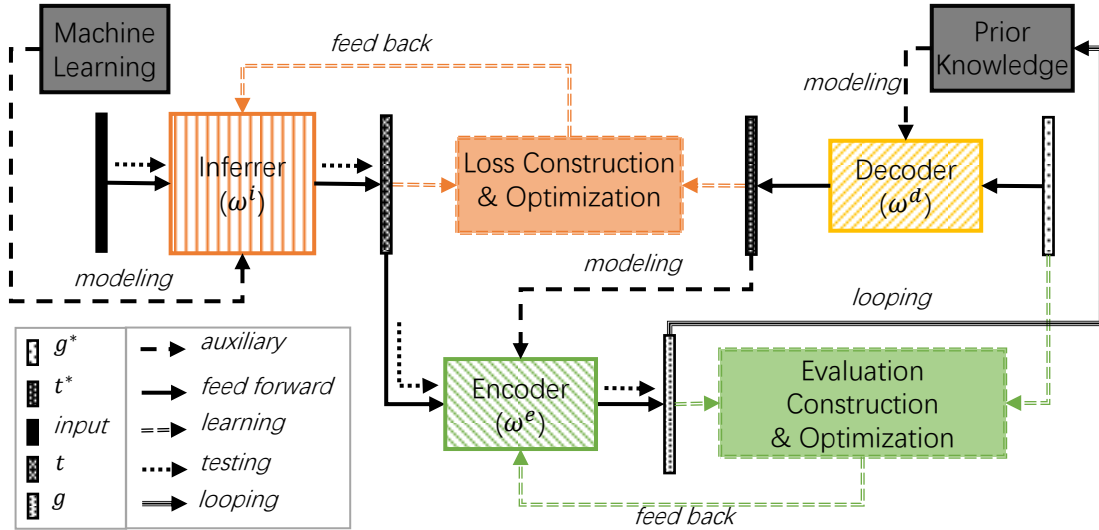


Fig. 3. Generalized MSL framework. Basic components: decoder, inferrer and encoder.

### 4.2.2 Basic procedure

**Learning** The learning procedure aims to optimize the parameters  $\omega^i$  and  $\omega^e$  for the inferrer and encoder, respectively, under the prerequisite of a decoder that is empirically initialized with  $\bar{\omega}^d$ . Specifically, we express the learning procedure as

$$\bar{t}^* = \text{decoder}(g^*; \bar{\omega}^d), \quad (4-1)$$

$$\bar{\omega}^i = \arg \min_{\omega^i \in M^i} \frac{1}{N} \sum_{n=1}^N \ell^i(\text{inferred}(d_n; \omega^i), \bar{t}_n^*), \quad (4-2)$$

$$\bar{\omega}^e = \arg \min_{\omega^e \in M^e} \frac{1}{N} \sum_{n=1}^N \ell^e(\text{encoder}(t_n; \omega^e), g_n^*), \quad (4-3)$$

where  $M^i$  and  $M^e$  specify the parameter spaces of  $\omega^i$  and  $\omega^e$ , respectively, and  $N$  is the number of training events/entities.

**Looping** As the optimization of the parameters ( $\omega^i$ ,  $\omega^e$ ) of both the inferrer and encoder is conducted under the prerequisite of the decoder parameterized by  $\omega^d$ , a change in the decoder can significantly affect the optimization of  $\omega^i$  and  $\omega^e$ , which will eventually be reflected in the final predicted labels  $g$ . In fact, prior knowledge can be enriched by analysing the predicted labels  $g$  of the current solution. The enriched prior knowledge can help us to model and initialize a better decoder. Thus, in practice, we commonly loop several times to adjust the decoder and restart the training for a possibly better solution. Specifically, we express the looping procedure as

$$\bar{\omega}^d = \arg \min_{\omega^d \in M^d} l(g|\omega^d, g^*), \quad (5)$$

where  $M^d$  signifies the parameter space of  $\omega^d$  and  $g|\omega^d$  denotes that the final predicted labels  $g$  are obtained by optimizing the parameters ( $\omega^i$ ,  $\omega^e$ ) of both the inferrer and encoder under the prerequisite of the decoder initialized with  $\omega^d$ .

**Testing** As shown in Fig. 2, testing starts from input  $d$ , passes through the inferrer and encoder, and ends at  $g$ . Specifically, the testing procedure can be expressed as

$$t = \text{inferred}(d; \bar{\omega}^i | \bar{\omega}^d), \quad (6-1)$$

$$g = \text{encoder}(t; \bar{\omega}^e | \bar{\omega}^d), \quad (6-2)$$

where  $\bar{\omega}^i | \bar{\omega}^d$  and  $\bar{\omega}^e | \bar{\omega}^d$  are the parameters of the inferrer and encoder optimized under the prerequisite of the decoder initialized with  $\bar{\omega}^d$  found by the looping procedure.

#### 4.2.3 Analysis

From Eq. (1) to (6), we can note that the generalized framework presented for MSL in fact reveals the key points of constructing fundamental MSL solutions and the key problems of developing better MSL solutions, which are concealed by the roughness of FSL category. The key points of constructing fundamental MSL solutions can be summarized as modelling the three basic components (decoder, inferrer and encoder), and the key problems of developing better MSL solutions can be summarized as the learning and looping procedures to optimize the three basic components. The decoder is responsible for transforming the given ground-truth labels into learnable targets. Usually, it is built and optimized on the basis of prior knowledge. The inferrer is responsible for mapping events/entities to corresponding learnable targets. Usually, it is built and optimized on the basis of machine learning techniques. The encoder is responsible for transforming the predicted targets of the inferrer into final predicted labels. Usually, the encoder is built and optimized on the basis of the decoder.

#### 4.3 Generality

Although solutions have been intermittently proposed for different MSL tasks, little work has explored the generality of different MSL tasks, due to the lack of a clear problem definition and

systematic problem analysis. In this subsection, based on the specified definition and presented framework for MSL, we show that generality exists among cell detection (CD) [3] and line segment detection (LSD) [4], which are two typical MSL tasks according to the definition of MSL and have large differences in application scenarios. Following the presented framework for MSL, we review and rebuild the solutions proposed in [3, 4] for these two largely different typical MSL problems to show that generality exist in their solutions.

#### 4.3.1 Cell detection

Let  $\mathcal{F}$  be a 2D image lattice (e.g.,  $800 \times 800$ ). The moderate supervision information for the CD task uses a point  $p_j = (x_j, y_j)$  with offsets  $x_j$  and  $y_j$ , respectively, to represent the cell centre in  $\mathcal{F}$ . In this situation, the ground-truth label in  $\mathcal{F}$  is denoted by  $P = \{p_j | j = \{1, \dots, m\}\}$ . Some example images and corresponding ground-truth labels are given in Fig. 4.

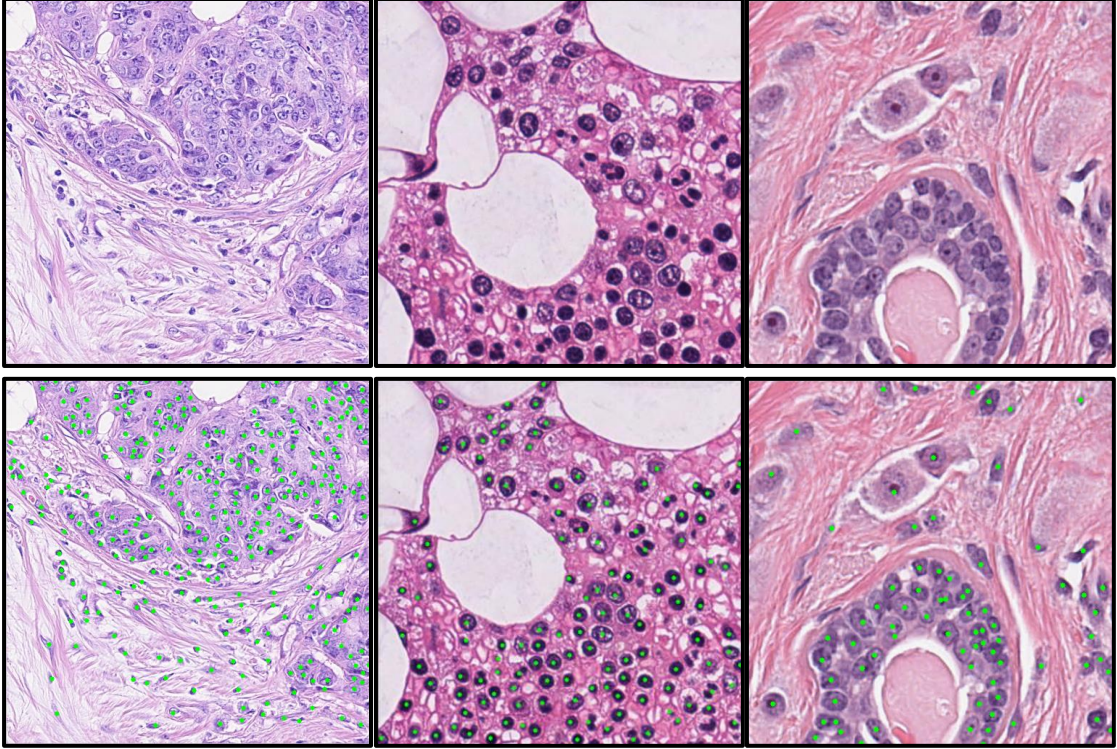


Fig. 4. Example images and corresponding ground-truth labels for cell detection [3, 37, 38]. Top row: original images. Bottom row: ground-truth labels shown on original images.

##### (1) Decoder

The decoder transforms  $P$  labelled in an image lattice  $\mathcal{F}$  into a structured learnable target. It first assigns each pixel point  $p \in \mathcal{F}$  to the nearest cell centre point in  $P$  to partitions  $\mathcal{F}$  into  $m$  regions. Each region serves as a supportive area for a cell centre point. Then, by projecting its supportive region into a 1D real-valued representation, it transforms each cell centre  $p_j$  in  $P$  into a structured representation.

**Modelling** For assignment of a pixel point  $p \in \mathcal{F}$  to its nearest cell centre point, we use Euclidian distance to define the distance between  $p$  and a candidate cell centre point  $p_j$  as

$$dis(p, p_j) = \sqrt{(p - p_j)^2} = \sqrt{(x - x_j)^2 + (y - y_j)^2}.$$

The supportive region for cell centre point  $p_j$  is denoted by

$$R(p_j) = \{p | p \in \mathcal{F}; \text{dis}(p, p_j) < \text{dis}(p, p_k), \forall k \neq j, p_k \in P\}.$$

Then, we define the transformation of each pixel point  $p$  in a supportive region  $R(p_j)$  into a real-valued representation by

$$a_j(p) = e^{\left(1 - \frac{\text{dis}(p, p_j)}{\text{dis}_j}\right)} - 1, \quad p \in R(p_j), \quad \text{dis}_j = \max \text{dis}(p, p_j).$$

Using  $a_j$ , we can transform a cell centre  $p_j$  into a structured 1D representation. This transformation function is applied over the entire  $P$  labelled in image lattice  $\mathcal{F}$  as

$$a: P \xrightarrow{\text{transforming}} \mathbb{R},$$

$$p_j \rightarrow a_j(R(p_j)), \quad p_j \in P.$$

For simplicity, the structured target generated by the transformation function  $a$  can be denoted by

$$E = \{a_j(R(p_j)) | p_j \in P; j = \{1, \dots, m\}\}.$$

**Parameterization** Using the transformation function  $a$ , we can transform  $P$  labelled in  $\mathcal{F}$  into a structured target without setting any specific parameters. However, the structured target transformed by this parameter-free model is redundant since many pixel points far from a line segment can also be assigned as being among its supportive points, which we believe is unnecessary. Note that  $\varphi$  is the parameter for adjusting the selection of necessary pixel points in  $\mathcal{F}$ . We parameterize and rewrite the supportive region for cell centre point  $p_j$  as

$$R(p_j; \varphi) = \begin{cases} R_+(p_j; \varphi) = \{p | p \in R(p_j); \text{dis}(p, p_j) < \varphi; \} \\ R_-(p_j; \varphi) = \{p | p \in R(p_j); \text{dis}(p, p_j) \geq \varphi; \} \end{cases}$$

Then, the function for transforming each pixel point  $p$  in  $R(p_j; \varphi)$  into a real-valued representation is rewritten as

$$a_j(p; \{\varphi, \alpha\}) = \begin{cases} e^{\alpha \left(1 - \frac{\text{dis}(p, p_j)}{\varphi}\right)} - 1 & \text{if } p \in R_+(p_j; \varphi), \\ 0 & \text{if } p \in R_-(p_j; \varphi) \end{cases}$$

where  $\alpha$  is a parameter added to control the exponential decrease rate of  $\varphi$  close to the centre point.

**Generalization** Decoding model:  $\{R, a\}$ ; Input:  $g^* = P$ ; Parameter:  $\omega^d = \{\varphi, \alpha\}$ ; Output:  $t^* = E$ . Referring to Eq. (1), the transforming process of the decoder for the CD task can be defined as

$$E = \underset{\{R, a\}}{\text{decoder}}(P; \{\varphi, \alpha\}). \quad (\text{CD-1})$$

Fig. 5 illustrates how the decoder transforms the ground-truth label into a learnable target for the CD task.

## (2) Inferer

**Modelling** A deep convolutional neural network (DCNN) is employed to model the inferer for mapping an input image lattice  $D$  to an indirect target  $G$ . Define  $\{f_o\}_{o=1}^O$  as the transformation for each of the  $O$  layers from the DCNN architecture. The mapping function of the inferer can be denoted by

$$\psi = f_o \circ f_{o-1} \circ \dots \circ f_1.$$

Given one input image lattice  $D$ , the network computes the output  $G$  as

$$G = \psi(D).$$

**Parameterization** We assume  $\{f_o\}_{o=1}^O$  are parameterized by  $\{\theta_o\}_{o=1}^O$ . The corresponding  $\theta_o$  has distinct forms for different types of  $f_o$ . The output computation of the network is rewritten by

$$G = \psi(D; \theta),$$

$$\theta = \{\theta_1, \dots, \theta_O\}.$$

**Generalization** Inferring model:  $\{\psi\}$ ; Input:  $d = D$ ; Parameter:  $\omega^i = \{\theta\}$ ; Output:  $t = G$ . Referring to Eq. (2), the Inferer for the CD task can be abbreviated as

$$G = \underset{\{\psi\}}{\text{inferer}}(D; \{\theta\}). \quad (\text{CD-2})$$

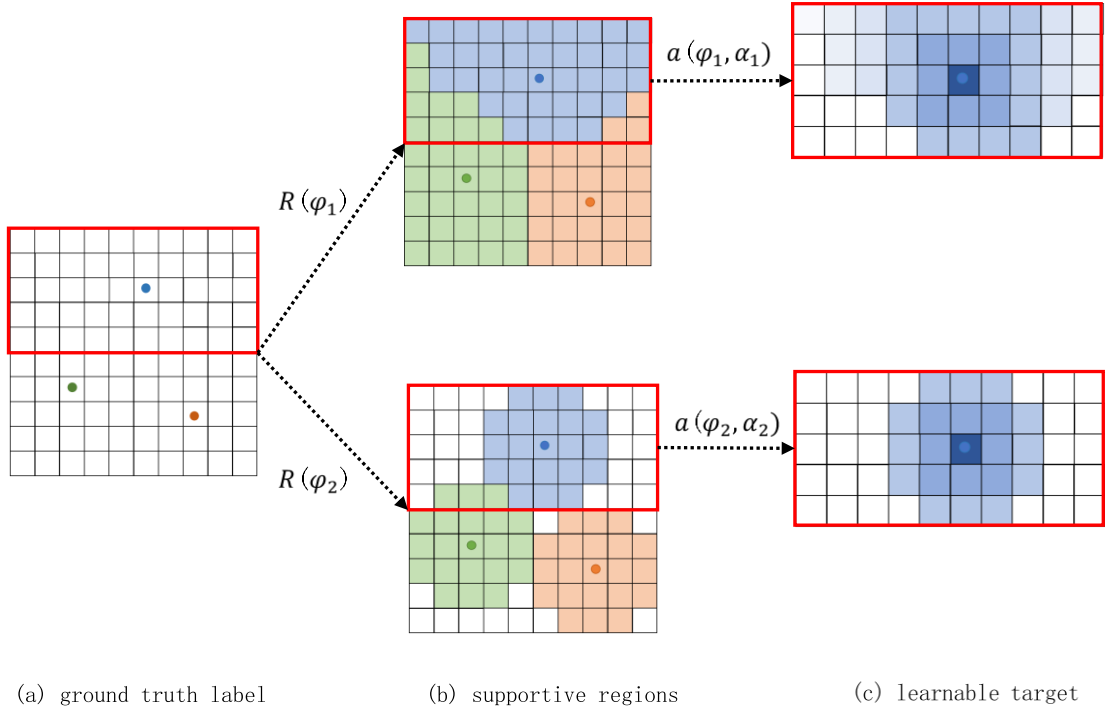


Fig. 5. Illustration of the transforming process of the decoder for the CD task. (a) The given ground-truth label is a  $10 \times 10$  image lattice in which the centres of three cells are labelled. (b) Supportive regions generated during the transforming process of the decoder. (c) Learnable target generated by transforming supportive regions into a structured representation. The top rows and bottom rows of (a) and (c) are two transformations of the decoder by adjusting its parameters.

### (3) Encoder

**Modelling** Since the decoder is built to respond maximally at the cell centres, the inferer is built to minimize the error between its output  $G$  and the output  $E$  of the decoder. Thus, by finding local maxima points in the lattice  $G$ , we can theoretically re-transform the structured prediction into the detected cell centres. For each point  $p = (x, y)$  in lattice  $G$ , we define  $p$  as a local maxima point if the values at its neighbours  $N = \{(x, y - 1), (x, y + 1), (x - 1, y), (x + 1, y)\}$  are smaller than or equal to the value at point  $p$ , which can be expressed as

$$\phi(p) = \begin{cases} p & \text{if } G(p) \geq G(p_n), \forall p_n \in N \\ (-1, -1) & \text{otherwise} \end{cases}$$

This re-transformation function is applied over the whole lattice  $G$

$$\phi: G \xrightarrow{\text{re-transforming}} \mathbb{R}^2,$$

$$p \rightarrow \phi(p), \quad p \in G.$$

As a result, the cell centres detected by the re-transformation function  $\phi$  can be denoted as

$$C = \{p | p \in G; \phi(p) \neq (-1, -1)\}.$$

**Parameterization** Since noise information appears in the raw output of the inferrer, we apply a small threshold  $\varepsilon \in [0, 1]$  to remove values smaller than  $\varepsilon \cdot \max(G)$ . We parameterize and rewrite the re-transformation function as

$$\phi(p, \varepsilon) = \begin{cases} \text{true} & \text{if } G(p) \geq \varepsilon \cdot \max(G) \cap G(p) \geq G(p_n), \forall p_n \in N \\ \text{false} & \text{otherwise} \end{cases}$$

Optimizing  $\varepsilon$  can balance between the recall and precision of the final cell detection.

**Generalization** Encoder model:  $\{\phi\}$ ; Input:  $t = G$ ; Parameter:  $\omega^e = \{\varepsilon\}$ ; Output:  $g = C$ . Referring to Eq. (3), the encoder for the CD task can be abbreviated as

$$C = \text{encoder}_{\{\phi\}}(G; \{\varepsilon\}). \quad (\text{CD-3})$$

#### (4) Learning

Referring to Eq. (4), in the learning procedure for the CD task, we first empirically initialize the decoder with  $\{\bar{\varphi}, \bar{\alpha}\}$  and utilize the initialized decoder to transform  $P$  labelled in an image lattice  $\mathcal{F}$  into a structured target by

$$\bar{E} = \text{decoder}_{\{R, \alpha\}}(P; \{\bar{\varphi}, \bar{\alpha}\}). \quad (\text{CD-4-1})$$

Then, we optimize the parameters of the inferrer by

$$\begin{aligned} \tilde{\theta} &= \arg \min_{\theta \in M^i} \frac{1}{N} \sum_{n=1}^N \ell^i \left( \text{inferrer}_{\{\psi\}}(D_n; \{\theta\}), \bar{E} \right), \\ \ell^i \left( \text{inferrer}_{\{\psi\}}(D; \{\theta\}), \bar{E} \right) &= \frac{1}{2} \sum_{p \in \mathcal{F}} (\beta G(p) + \gamma \bar{G})(G(p) - \bar{E}(p)), \end{aligned} \quad (\text{CD-4-2})$$

where  $\beta$  and  $\gamma$  are predefined constants used to tune the losses. The parameters of the encoder are optimized by

$$\begin{aligned} \tilde{\varepsilon} &= \arg \min_{\varepsilon \in M^e} \frac{1}{N} \sum_{n=1}^N \ell^e \left( \text{encoder}_{\{\phi\}}(C_n; \{\varepsilon\}), P_n \right), \\ \ell^e \left( \text{encoder}_{\{\phi\}}(C; \{\varepsilon\}), P \right) &= \frac{(C \cup P) - (C \cap P)}{C \cup P}. \end{aligned} \quad (\text{CD-4-3})$$

#### (5) Looping

Usually, we loop several times to find relatively optimal parameters for the decoder. Referring to Eq. (5), the looping procedure for the CD task can be specified as

$$\begin{aligned} \{\tilde{\varphi}, \tilde{\alpha}\} &= \arg \min_{\{\varphi, \alpha\} \in M^d} l(C | \{\varphi, \alpha\}, P), \\ l(C | \{\varphi, \alpha\}, P) &= \frac{((C | \{\varphi, \alpha\}) \cup P) - ((C | \{\varphi, \alpha\}) \cap P)}{(C | \{\varphi, \alpha\}) \cup P}, \\ C | \{\varphi, \alpha\} &= \text{encoder}_{\{\phi\}} \left( \text{inferrer}_{\{\psi\}}(D; \{\tilde{\theta}\}); \{\tilde{\varepsilon}\} \right). \end{aligned} \quad (\text{CD-5})$$

#### (6) Testing

Referring to Eq. (6), the testing procedure for the CD task can be specified as

$$G = \text{inferrer}_{\{\psi\}}(D; \{\tilde{\theta}\} | \{\tilde{\varphi}, \tilde{\alpha}\}), \quad (\text{CD-6-1})$$



$$C = \text{encoder}_{\{\phi\}}(G; \{\tilde{\varepsilon}\}|\{\tilde{\phi}, \tilde{\alpha}\}). \quad (\text{CD-6-2})$$

#### 4.3.2 Line segment detection

Let  $\mathcal{F}$  be a 2D image lattice (e.g.,  $800 \times 800$ ). The moderate supervision information for the LSD task uses  $l_k = (p_k^s, p_k^e)$  with the two points  $p_k^s = (x_k^s, y_k^s)$  and  $p_k^e = (x_k^e, y_k^e)$  representing the position of a line segment in  $\mathcal{F}$ . In this situation, the ground-truth label for  $\mathcal{F}$  is denoted by  $L = \{l_k | k = \{1, \dots, m\}\}$ . Some example images and corresponding ground-truth labels are given in Fig. 6.

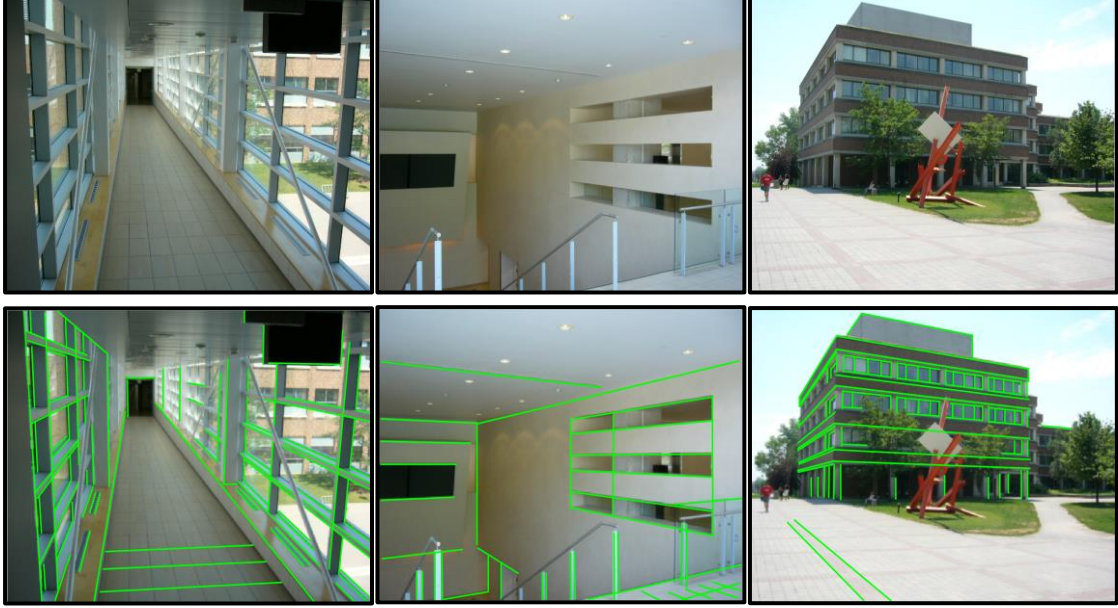


Fig. 6. Example images and corresponding ground-truth labels for line segment detection [39, 40]. Top row: original images. Bottom row: ground-truth labels shown on original images.

##### (1) Decoder

The decoder transforms line segments  $L$  labelled in an image lattice  $\mathcal{F}$  into a structured learnable target. It first assigns each pixel point  $p \in \mathcal{F}$  to the nearest line segment in  $L$ , which partitions  $\mathcal{F}$  into  $m$  regions. Each region serves as a supportive area for a line segment. Then, by projecting its supportive region into a 2D real-valued representation, each line segment  $l_j$  in  $L$  is transformed into a structured representation.

**Modelling** For the assignment of a pixel point  $p \in \mathcal{F}$  to its nearest line segment, we use a distance function that defines the shortest distance between  $p$  and a candidate line segment  $l_k$  as

$$\text{dis}(p, l_k) = \min_{z \in [0,1]} \text{dis}(p, l_k; z) = \min_{z \in [0,1]} \|p_k^s + z \cdot (p_k^e - p_k^s) - p\|_2^2.$$

The value of  $t$  associated with the shortest distance between  $p$  and  $l_k$  is defined as

$$z_p^\sim = \arg \min_{z \in [0,1]} \text{dis}(p, l_k; z).$$

The projection point  $p'$  of  $p$  on  $l_k$  is defined as

$$p' = p_k^s + z_p^\sim \cdot (p_k^e - p_k^s).$$

The supportive region for line segment  $l_k$  is defined as



$$R(l_k) = \{p | p \in \mathcal{F}; \text{dis}(p, l_k) < \text{dis}(p, l_j), \forall j \neq k, l_j \in L\}.$$

Then, the transformation of each pixel point  $p$  in a supportive region  $R(l_k)$  into a structured 2D representation is defined by

$$a_k(p) = p' - p, \quad p \in R(l_k)$$

where the 2D representation vector is perpendicular to the line segment  $l_k$  when  $t_p \in (0,1)$ .

This transformation function is applied over the whole  $L$  labelled in image lattice  $\mathcal{F}$  as

$$a: L \xrightarrow{\text{transforming}} \mathbb{R}^2,$$

$$l_k \rightarrow a_k(R(l_k)), \quad l_k \in L.$$

For simplicity, the structured target generated by the transformation function  $a$  can be denoted by

$$E = \{a_k(R(l_k)) | l_k \in L; k = \{1, \dots, m\}\}.$$

**Parameterization** Using the transformation function  $a$ , we can transform  $L$  labelled in  $\mathcal{F}$  into a structured target without setting any specific parameters. However, the structured target transformed by this parameter-free model is redundant since many pixel points far from a line segment can also be assigned as its supportive points, which we believe is unnecessary. Note that  $\varphi$  is the parameter for adjusting the selection of necessary pixel points in  $\mathcal{F}$ . We parameterize and rewrite the supportive region for line segment  $l_k$  as

$$R(l_k; \varphi) = \begin{cases} R_+(l_k; \varphi) = \{p | p \in R(l_k); d(p, l_k) < \varphi\} \\ R_-(l_k; \varphi) = \{p | p \in R(l_k); d(p, l_k) \geq \varphi\} \end{cases}.$$

Then, the transformation of each pixel point  $p$  in a supportive region  $R(l_k; \varphi)$  into a structured 2D representation is defined as

$$a_k(p) = \begin{cases} p' - p & p \in R_+(l_k; \varphi) \\ (-x - 1, -y - 1), & p \in R_-(l_k; \varphi) \end{cases}.$$

**Generalization** decoder model:  $\{R, a\}$ ; Input:  $g^* = L$ ; Parameter:  $\omega^d = \varphi$ ; Output:  $t^* = A$ . Referring to Eq. (1), we abbreviate the transforming process of the decoder for the LSD task as

$$E = \text{decoder}(L; \varphi)_{\{R, a\}}.$$

(LSD-1)

Fig. 7 illustrates how the decoder transforms the ground-truth label into a learnable target for the LSD task.

## (2) Inferer

A DCNN is employed to model the inferer for mapping an input image lattice  $D$  to an indirect target  $G$ , which can be denoted as

$$G = \text{inferer}(D; \{\theta\})_{\{\psi\}}, \quad (\text{LSD-2})$$

where  $\psi$  is the mapping function of the inferer and  $\theta$  are the parameters of  $\psi$ .

## (3) Encoder

**Modelling** For each pixel point  $p$  in  $G$ , we can compute its predicted projection point on a possible line segment by

$$v(p) = p + G(p),$$

where  $G(p)$  denotes the predicted 2D vector at pixel point  $p$  of  $G$ . Its discretized point in the lattice is denoted by

$$v_\wedge(p) = \lfloor v(p) + 0.5 \rfloor,$$

where  $\lfloor \cdot \rfloor$  represents the floor operation. In addition, if the projected point  $v(p)$  is inside a line segment,  $G(p)$  provides the normal direction of the line segment going through the point  $v(p)$

$$\tau(p) = \arctan2(G_x(p), G_y(p)).$$

Using  $v_\lambda(p)$ , we can rearrange  $G$  into a sparse map that records the locations of possible line segments. Such a sparse map is termed a line proposal map, in which a pixel point  $q$  collects supportive pixels whose discretized projection points are  $q$ . The candidate set of supportive pixels collected by pixel  $q$  in the line proposal map is defined by

$$S(q) = \{G(p) | p \in G, v_\lambda(p) = q\}.$$

Thus, using  $C(q)$ , a line proposal map is defined by

$$Q = \{q | S(q) \neq \emptyset, \forall q \in \mathcal{F}\}.$$

where each pixel point  $q$  of  $Q$  corresponds to a point on a possible line segment and is associated with a set of supportive pixels  $C(q)$  in  $G$ . The line proposal map projects the supportive pixels for a line segment into pixels near the line segment.

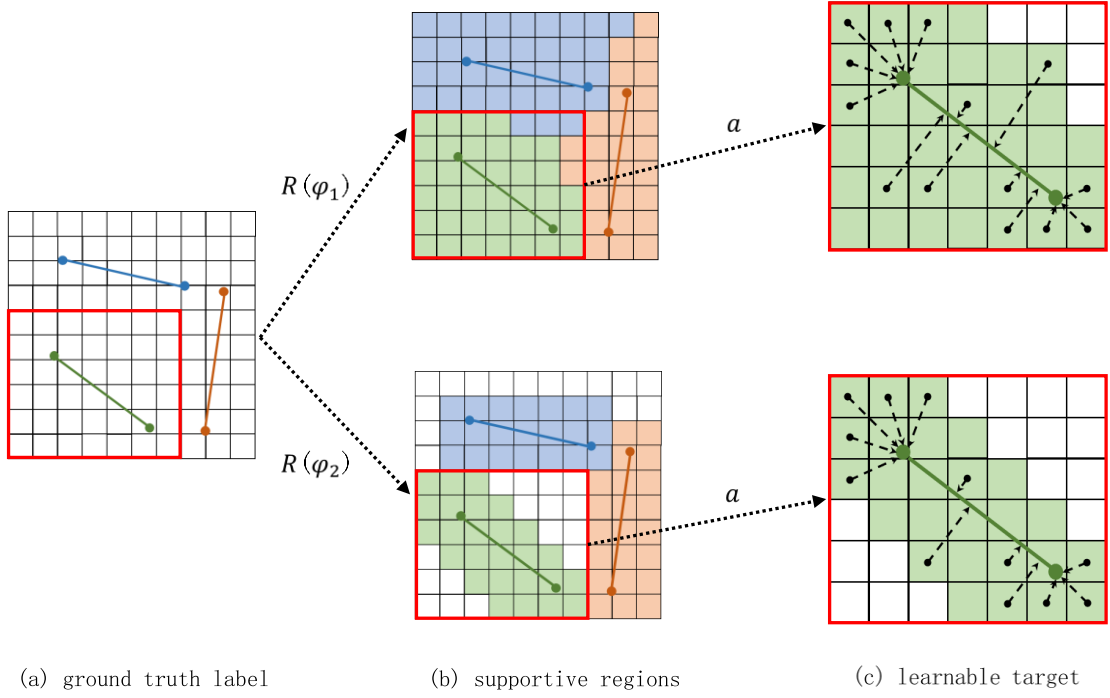


Fig. 7. Illustration of the transforming process of the decoder for the LSD task. (a) The given ground-truth label is a  $10 \times 10$  image lattice in which the ends of three line-segments are labelled. (b) Supportive regions generated during the transformation process of the decoder. (c) Learnable target generated by transforming supportive regions into a structured representation. The top rows and bottom rows of (a) and (c) are two transformations of the decoder obtained by adjusting its parameters.

With the line proposal map  $Q$ , the problem is to group the points of  $Q$  into line segments to eventually re-transform the structured prediction into detected line segments. In the spirit of the region growing algorithm used in [41], an iterative and greedy grouping strategy is employed to fit line segments. The procedures of this strategy are as follows.

First, from the line proposal map  $Q$ , we obtain the current set of active pixels, each of which

has a non-empty candidate set of supportive pixels. We also randomly select a pixel from the set of active pixels and obtain its supportive pixels. This procedure can be denoted by

$$q_0 = \text{random\_selection}(Q),$$

$$c_0 = C(q_0).$$

Second, with  $Q$ ,  $q_0$ , and  $c_0$ , we initialize the points of the current line segment and its supportive pixels and deactivate the points of the current line from  $Q$ , which can be denoted by

$$q_c = \{q_0\},$$

$$c_c = \{c_0\},$$

$$Q = \text{deactive}(Q, q_0).$$

Iteratively, from  $Q$ , we find more active pixels that are aligned with the current line segment and group these active pixels aligned with points of the current line segment, which can be denoted by

$$s = \text{center\_align}(Q, q_c, c_c),$$

$$\text{group}(q_c, c_c, s) \Rightarrow \begin{cases} \text{end} & s = \emptyset \\ \begin{cases} q_c = q_c \cup s \\ c_c = c_c \cup C(s) \\ Q = \text{deactive}(Q, s) \end{cases} & \text{otherwise} \end{cases}$$

Finally, we fit the minimum outer rectangle of  $q_c$  to obtain the current line segment, which can be denoted by

$$(p_{q_c}^s, p_{q_c}^e) = \text{rectangle}(q_c),$$

$$l_{q_c} = (p_{q_c}^s, p_{q_c}^e).$$

This grouping strategy is applied over  $Q$  until all of its pixels are inactive. Denote the above procedures as  $\phi = \{\text{cente\_align}, \text{group}, \text{rectangle}\}$ , the re-transformation function can be expressed as

$$\phi: G \xrightarrow{\text{re-transforming}} (\mathbb{R}^2, \mathbb{R}^2),$$

$$G \rightarrow \phi(G).$$

As a result, the line segments detected using the re-transformation function  $\phi$  can be denoted by

$$C = \{l_{q_c} | q_c \in Q\}.$$

**Parameterization** We can parameterize the *center\_align* model by searching the local observation window (e.g.,  $r_{w \times w}$ , a  $w \times w$  window is used) centred at  $q_c$  and finding more active pixels that are aligned with points of the current line segment with an angular distance less than a threshold (e.g.,  $\tau_d = 10^\circ$ ). Thus, we parameterize and rewrite *center\_align* as

$$s = \text{center\_align}(Q, q_c, c_c; r_{w \times w}, \tau_d).$$

To verify the candidate line segment, we can check the aspect ratio between the width and height of the approximated rectangle with respect to a predefined threshold (e.g.,  $r_{w/h}$ ) to ensure that the approximated rectangle is sufficiently thin. As a result, we parameterize and rewrite *rectangle* as

$$(p_{q_c}^s, p_{q_c}^e) = \text{rectangle}(q_c; r_{w/h}),$$

$$l_q = \begin{cases} \text{null} \\ Q_a = \text{reactivate}(Q_a, (q_c - q_0)) \end{cases} \quad \text{if } (p_{q_c}^s, p_{q_c}^e) == (\text{null}, \text{null}),$$

$$(p_{q_c}^s, p_{q_c}^e) \quad \text{otherwise}$$

in which if the verification fails, we keep  $q_0$  inactive and reactivate  $(q_c - q_0)$ .

**Generalization** Encoder model:  $\phi = \{\text{cente\_align}, \text{group}, \text{rectangle}\}$ ; Input:  $t = G$ ;

Parameter:  $\omega^e = \varepsilon = \{r_{w \times w}, \tau_d, r_{w/h}\}$ ; Output:  $g = C$ . Referring to Eq. (3), the encoder for the LSD task can be abbreviated as

$$C = \text{encoder}_{\{\phi\}}(G; \{\varepsilon\}). \quad (\text{LSD-3})$$

#### (4) Learning

Referring to Eq. (4), in the learning procedure for the LSD task, we can empirically initialize the decoder with  $\{\bar{\varphi}\}$  and utilize the initialized decoder to transform  $L$  labelled in an image lattice  $\mathcal{F}$  into a structured target by

$$\bar{E} = \text{decoder}_{\{R, a\}}(L; \{\bar{\varphi}\}). \quad (\text{LSD-4-1})$$

Then, we optimize the parameters of the inferrer by

$$\begin{aligned} \tilde{\theta} &= \arg \min_{\theta \in M^i} \frac{1}{N} \sum_{n=1}^N \ell^i \left( \text{inferrer}_{\{\psi\}}(D_n; \{\theta\}), \bar{E} \right), \\ \ell^i \left( \text{inferrer}_{\{\psi\}}(D; \{\theta\}), \bar{E} \right) &= \sum_{p \in \mathcal{F}} \|\bar{E}(p) - G(p)\|_1. \end{aligned} \quad (\text{LSD-4-2})$$

Then, we optimize the parameters of the encoder by

$$\begin{aligned} \tilde{\varepsilon} &= \arg \min_{\varepsilon \in M^e} \frac{1}{N} \sum_{n=1}^N \ell^e \left( \text{encoder}_{\{\phi\}}(C_n; \{\varepsilon\}), L_n \right), \\ \ell^e \left( \text{encoder}_{\{\phi\}}(C; \{\varepsilon\}), L \right) &= \frac{(C \cup L) - (C \cap L)}{C \cup L}. \end{aligned} \quad (\text{LSD-4-3})$$

#### (5) Looping

Usually, we loop several times to find relatively optimal parameters for the decoder. Referring to Eq. (5), the looping procedure for the LSD task can be defined as

$$\begin{aligned} \{\tilde{\varphi}\} &= \arg \min_{\{\varphi\} \in M^d} l(C|\{\varphi\}, L), \\ l(C|\{\varphi\}, L) &= \frac{((C|\{\varphi\}) \cup L) - ((C|\{\varphi\}) \cap L)}{(C|\{\varphi\}) \cup L}, \\ C|\{\varphi\} &= \text{encoder}_{\{\phi\}} \left( \text{inferrer}_{\{\psi\}}(D; \{\tilde{\theta}\}); \{\tilde{\varepsilon}\} \right). \end{aligned} \quad (\text{LSD-5})$$

#### (6) Testing

Referring to Eq. (6), the testing procedure for the LSD task can be defined as

$$G = \text{inferrer}_{\{\psi\}}(D; \{\tilde{\theta}\}|\{\tilde{\varphi}\}), \quad (\text{LSD-6-1})$$

$$C = \text{encoder}_{\{\phi\}}(G; \{\tilde{\varepsilon}\}|\{\tilde{\varphi}\}). \quad (\text{LSD-6-2})$$

### 4.3.3 Analysis

From the rebuilt solutions presented in section 4.3.1 and section 4.3.2 for the CD and LSD tasks, we draw a summarization as Fig. 8. From Fig. 8 we can note that the two solutions for the CD and LSD tasks can be abstractly expressed as the form of the MSL framework presented in section 4.2, though they have large differences in detailed implementations. In other words, by simply comparing the detailed implementations of the two solutions for CD and LSD, it is hard for one to instantly say that the two solutions intrinsically share the same methodological formation. However, by referring to the definition and framework presented for MSL, it is easy for one to say that the two solutions for CD and LSD intrinsically share the same methodological formation. This

proves that generality exist in different MSL solutions, which have large differences, when we view them from an abstract point of view; that is, solutions for a wide variety of MSL tasks can probably be unified into the same abstract formulation.

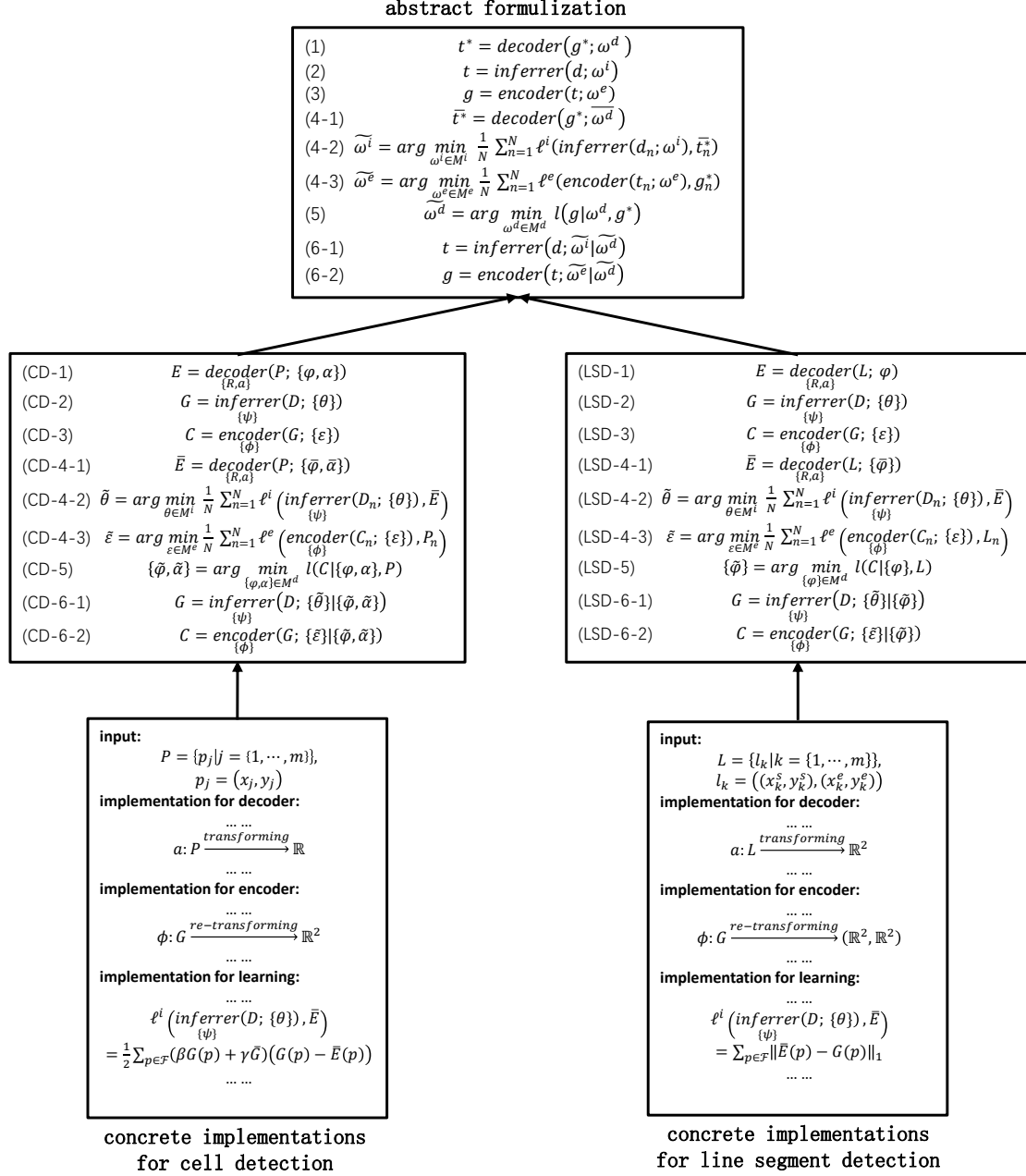


Fig. 8. Summarization of the rebuilt solutions for the CD and LSD tasks.

## 5. Discussion

In the current literature, by referring to the properties of the ground-truth labels prepared for the training data set, supervised learning is roughly categorized as fully supervised learning (FSL), which concerns the situation where the training data set is assigned with ideal ground-truth labels, and weakly supervised learning (WSL), which concerns the situation where the training data set is

assigned with non-ideal ground-truth labels. In this paper, we argue that the roughness of FSL category conceals some details that are critical to building the appropriate solutions for some specific FSL tasks, noticing the target transformation from the given ground-truth labels to learnable targets can significantly affect the performance of the final FSL solutions. Taking into consideration the properties of the target transformation from the given ground-truth labels to learnable targets, we firstly categorize FSL into three narrower sub-types including: precisely supervised learning (PSL), which concerns the situation where the given ground-truth labels are precisely fine; moderately supervised learning (MSL), which concerns the situation where the given ground-truth labels are ideal, but due to the simplicity in annotation of the given ground-truth labels, careful designs are required to transform the given ground-truth labels into learnable targets for the learning task; and precisely and moderately combined supervised learning (PMCSL) which concerns the situation where the given ground-truth labels contain both precise and moderate annotations. Then we focus on the MSL subtype and comprehensively illustrate MSL from the perspectives of the definition, framework and generality to reveal what details are concealed by the roughness of the FSL category.

Primarily, we present the definition of MSL that proves that some details are indeed concealed by the roughness of FSL category. Subsequently, based on the presented definition of MSL, we present the framework of MSL that reveals the key points of constructing fundamental MSL solutions and the key problems of developing better MSL solutions, which are critical to building the appropriate solutions but concealed by the roughness of FSL category. Finally, analyses of the methodologies for two largely different MSL tasks (cell detection and line segment detection) prove that generality exist in different MSL solutions when we view them from an abstract point of view; that is, solutions for a wide variety of MSL tasks can probably be unified into the same abstract formation.

Specifically, the key points of constructing fundamental MSL solutions can be summarized as modelling three basic components including decoder, inferrer and encoder, and the key problems of developing better MSL solutions can be summarized as the learning and looping procedures to optimize the three basic components. The decoder, which is usually built and optimized on the basis of prior knowledge, is responsible for transforming the given ground-truth labels into learnable targets. The inferrer, which is usually built and optimized on the basis of machine learning techniques, is responsible for mapping events/entities to corresponding learnable targets. The encoder, which is usually built and optimized on the basis of the decoder, is responsible for transforming the predicted targets of the inferrer into final predicted labels. While abundant modelling approaches [45–48] and optimization methods [49–51] have been proposed for the inferrer, the modelling and optimization of the decoder and the encoder lack systematic and comprehensive studies, except for some sporadic solutions for specific MSL tasks [3–6]. On one hand, although successful decoders [3–6] have been proposed for different MSL tasks, the general methodology for modelling an appropriate decoder for an MSL task is still unclear. As the decoder determines how an MSL task is defined and is the prerequisite for optimization of both the inferrer and decoder, it is valuable to investigate how to efficiently and effectively model a decoder for an MSL task with prior knowledge. On the other hand, because it is coupled with the decoder, small changes in the encoder can also significantly affect the final performance [3, 4, 52, 53]. Thus, it would also be interesting to investigate how to find an appropriate decoder for an MSL task. Respectively being the pre-processing and post-processing for the inferrer, the decoder and the

encoder both are critical to building the appropriate solutions for MSL tasks, especially when the current state-of-the-art inferrer (deep neural networks from complex [8, 23–27] to lightweight [42–44]) has been becoming standardized and reaching its limits in many AI applications.

One significance of this paper is that, with the definition and framework presented for MSL, it provides the fundamental basis to systematically analyse MSL that concerns the situation where the given ground-truth labels are ideal, but due to the simplicity in annotation of the given ground-truth labels, careful designs are required to transform the given ground-truth labels into learnable targets. Moreover, with the generality presented for MSL, it has been shown that the solutions for different MSL tasks can be unified into the same abstract formation though they have large differences in concrete implementations, which proves that a generality can probably exist among a wide variety of MSL tasks. Thus, the other significance of this paper is that it presents a tutorial for learning to view a problem to be solved from the mathematician's vision, which can be helpful for AI application engineers to discover, evaluate and select appropriate solutions for a problem to be solved.

## Reference

1. LeCun Y, Bengio Y, Hinton G (2015) Deep learning. *Nature* 521:436–444. <https://doi.org/10.1038/nature14539>
2. Zhou Z-H (2018) A brief introduction to weakly supervised learning. *Natl Sci Rev* 5:44–53. <https://doi.org/10.1093/nsr/nwx106>
3. Xie Y, Xing F, Shi X, et al (2018) Efficient and robust cell detection: A structured regression approach. *Med Image Anal* 44:245–254. <https://doi.org/10.1016/j.media.2017.07.003>
4. Xue N, Bai S, Wang F-D, et al (2019) Learning Regional Attraction for Line Segment Detection. *IEEE Trans Pattern Anal Mach Intell*. <https://doi.org/10.1109/tpami.2019.2958642>
5. Lin TY, Dollár P, Girshick R, et al (2017) Feature pyramid networks for object detection. In: *Proceedings - 30th IEEE Conference on Computer Vision and Pattern Recognition, CVPR 2017*
6. Lin TY, Goyal P, Girshick R, et al (2020) Focal Loss for Dense Object Detection. *IEEE Trans Pattern Anal Mach Intell*. <https://doi.org/10.1109/TPAMI.2018.2858826>
7. Law H, Deng J (2020) CornerNet: Detecting Objects as Paired Keypoints. *Int J Comput Vis*. <https://doi.org/10.1007/s11263-019-01204-1>
8. Krizhevsky A, Sutskever I, Hinton GE (2012) ImageNet Classification with Deep Convolutional Neural Networks. In: *Advances in Neural Information Processing Systems*. pp 1097–1105
9. Ghosh S, Das N, Das I, Maulik U (2019) Understanding deep learning techniques for image segmentation. *ACM Comput Surv*. <https://doi.org/10.1145/3329784>
10. Zhao ZQ, Zheng P, Xu ST, Wu X (2019) Object Detection With Deep Learning: A Review. *IEEE Trans. Neural Networks Learn. Syst*.
11. Ranjan R, Patel VM, Chellappa R (2019) HyperFace: A Deep Multi-Task Learning Framework for Face Detection, Landmark Localization, Pose Estimation, and Gender Recognition. *IEEE Trans Pattern Anal Mach Intell*. <https://doi.org/10.1109/TPAMI.2017.2781233>
12. Cao Z, Hidalgo Martinez G, Simon T, et al (2019) OpenPose: Realtime Multi-Person 2D Pose Estimation using Part Affinity Fields. *IEEE Trans Pattern Anal Mach Intell*.

- <https://doi.org/10.1109/tpami.2019.2929257>
13. Zhang J (2016) *Mathematicians' vision* (in Chinese). Hubei Science and Technology Press, Wuhan
  14. Yang Y, Wu Y, Chen N (2019) Explorations on visual localization from active to passive. *Multimed Tools Appl* 78:2269–2309. <https://doi.org/10.1007/s11042-018-6347-0>
  15. Yang Y, Chen N, Jiang S (2018) Collaborative strategy for visual object tracking. *Multimed Tools Appl* 77:7283–7303. <https://doi.org/10.1007/s11042-017-4633-x>
  16. Yang Y, Lv H, Chen N, et al (2020) FTBME: feature transferring based multi-model ensemble. *Multimed Tools Appl* 79:18767–18799. <https://doi.org/10.1007/s11042-020-08746-4>
  17. Yang Y, Lv H, Chen N, et al (2021) Local minima found in the subparameter space can be effective for ensembles of deep convolutional neural networks. *Pattern Recognit* 109:107582. <https://doi.org/10.1016/j.patcog.2020.107582>
  18. Zhou ZH (2018) A brief introduction to weakly supervised learning. *Natl. Sci. Rev.*
  19. Settles B (2010) Active Learning Literature Survey. *Mach Learn.* <https://doi.org/10.1.1.167.4245>
  20. Zhu X (2008) Semi-Supervised Learning Literature Survey Contents. *Sci York.* <https://doi.org/10.1.1.146.2352>
  21. Foulds J, Frank E (2010) A review of multi-instance learning assumptions. *Knowl. Eng. Rev.*
  22. Frénay B, Verleysen M (2014) Classification in the presence of label noise: A survey. *IEEE Trans Neural Networks Learn Syst.* <https://doi.org/10.1109/TNNLS.2013.2292894>
  23. Simonyan K, Zisserman A (2015) Very deep convolutional networks for large-scale image recognition. In: 3rd International Conference on Learning Representations, ICLR 2015 - Conference Track Proceedings
  24. Szegedy C, Ioffe S, Vanhoucke V, Alemi AA (2017) Inception-v4, inception-ResNet and the impact of residual connections on learning. In: 31st AAAI Conference on Artificial Intelligence, AAAI 2017
  25. He K, Zhang X, Ren S, Sun J (2016) Deep Residual Learning for Image Recognition. In: 2016 IEEE Conference on Computer Vision and Pattern Recognition (CVPR). IEEE, pp 770–778
  26. Huang G, Liu Z, Maaten L van der, Weinberger KQ (2017) Densely Connected Convolutional Networks. In: 2017 IEEE Conference on Computer Vision and Pattern Recognition (CVPR). IEEE, pp 2261–2269
  27. Hu J, Shen L, Sun G (2018) Squeeze-and-Excitation Networks. In: 2018 IEEE/CVF Conference on Computer Vision and Pattern Recognition. IEEE, pp 7132–7141
  28. Redmon J, Divvala S, Girshick R, Farhadi A (2016) You only look once: Unified, real-time object detection. In: Proceedings of the IEEE Computer Society Conference on Computer Vision and Pattern Recognition
  29. Redmon J, Farhadi A (2017) YOLO9000: Better, faster, stronger. In: Proceedings - 30th IEEE Conference on Computer Vision and Pattern Recognition, CVPR 2017
  30. Redmon J, Farhadi A (2017) Yolov3. *Proc IEEE Comput Soc Conf Comput Vis Pattern Recognit.* <https://doi.org/10.1109/CVPR.2017.690>
  31. Bochkovskiy A, Wang C-Y, Liao H-YM (2020) YOLOv4: Optimal Speed and Accuracy of Object Detection. *arXiv.org*
  32. Liu W, Anguelov D, Erhan D, et al (2016) SSD: Single Shot MultiBox Detector. In: ECCV 2016
  33. Girshick R, Donahue J, Darrell T, Malik J (2014) Rich feature hierarchies for accurate object



- detection and semantic segmentation. In: Proceedings of the IEEE Computer Society Conference on Computer Vision and Pattern Recognition
34. He K, Zhang X, Ren S, Sun J (2015) Spatial Pyramid Pooling in Deep Convolutional Networks for Visual Recognition. *IEEE Trans Pattern Anal Mach Intell*. <https://doi.org/10.1109/TPAMI.2015.2389824>
  35. Girshick R (2015) Fast R-CNN. In: Proceedings of the IEEE International Conference on Computer Vision
  36. Ren S, He K, Girshick R, Sun J (2017) Faster R-CNN: Towards Real-Time Object Detection with Region Proposal Networks. *IEEE Trans Pattern Anal Mach Intell*. <https://doi.org/10.1109/TPAMI.2016.2577031>
  37. Sirinukunwattana K, Raza SEA, Tsang YW, et al (2016) Locality Sensitive Deep Learning for Detection and Classification of Nuclei in Routine Colon Cancer Histology Images. *IEEE Trans Med Imaging*. <https://doi.org/10.1109/TMI.2016.2525803>
  38. Kainz P, Urschler M, Schultze S, et al (2015) You should use regression to detect Cells. In: *Lecture Notes in Computer Science (including subseries Lecture Notes in Artificial Intelligence and Lecture Notes in Bioinformatics)*
  39. Matas J, Galambos C, Kittler J (2000) Robust detection of lines using the progressive probabilistic hough transform. *Comput Vis Image Underst*. <https://doi.org/10.1006/cviu.1999.0831>
  40. Denis P, Elder JH, Estrada FJ (2008) Efficient edge-based methods for estimating manhattan frames in urban imagery. In: *Lecture Notes in Computer Science (including subseries Lecture Notes in Artificial Intelligence and Lecture Notes in Bioinformatics)*
  41. von Gioi RG, Jakubowicz J, Morel J-M, Randall G (2010) LSD: A Fast Line Segment Detector with a False Detection Control. *IEEE Trans Pattern Anal Mach Intell* 32:722–732. <https://doi.org/10.1109/TPAMI.2008.300>
  42. Howard A, Sandler M, Chen B, et al (2019) Searching for mobileNetV3. In: Proceedings of the IEEE International Conference on Computer Vision
  43. Sun K, Li M, Liu D, Wang J (2019) IGCv3: Interleaved low-rank group convolutions for efficient deep neural networks. In: *British Machine Vision Conference 2018, BMVC 2018*
  44. Zhang X, Zheng H, Sun J (2018) ShuffleNetV2. *ECCV*
  45. Shelhamer E, Long J, Darrell T (2017) Fully Convolutional Networks for Semantic Segmentation. *IEEE Trans Pattern Anal Mach Intell* 39:640–651. <https://doi.org/10.1109/TPAMI.2016.2572683>
  46. Badrinarayanan V, Kendall A, Cipolla R (2017) SegNet: A Deep Convolutional Encoder-Decoder Architecture for Image Segmentation. *IEEE Trans Pattern Anal Mach Intell* 39:2481–2495. <https://doi.org/10.1109/TPAMI.2016.2644615>
  47. Chen L-C, Papandreou G, Kokkinos I, et al (2018) DeepLab: Semantic Image Segmentation with Deep Convolutional Nets, Atrous Convolution, and Fully Connected CRFs. *IEEE Trans Pattern Anal Mach Intell* 40:834–848. <https://doi.org/10.1109/TPAMI.2017.2699184>
  48. Falk T, Mai D, Bensch R, et al (2019) U-Net: deep learning for cell counting, detection, and morphometry. *Nat Methods*. <https://doi.org/10.1038/s41592-018-0261-2>
  49. Bottou L (2010) Large-Scale Machine Learning with Stochastic Gradient Descent. In: *Proceedings of COMPSTAT'2010*
  50. Duchi J, Hazan E, Singer Y (2011) Adaptive subgradient methods for online learning and

- stochastic optimization. J Mach Learn Res
51. Kingma DP, Ba JL (2015) Adam: A method for stochastic gradient descent. ICLR Int Conf Learn Represent
  52. Bodla N, Singh B, Chellappa R, Davis LS (2017) Improving Object Detection With One Line of Code Navaneeth. Proc IEEE Int Conf Comput Vis. <https://doi.org/10.1109/ICCV.2017.593>
  53. Hosang J, Benenson R, Schiele B (2017) Learning non-maximum suppression. In: Proceedings - 30th IEEE Conference on Computer Vision and Pattern Recognition, CVPR 2017